Structural and Functional Investigations on Diiron Complexes: Catalase-Like Activity and Mechanistic Studies on the Formation of (μ-Peroxo)diiron(III) Adducts

Roberto Than,[a] Antje Schrodt,[b] Lars Westerheide,[a] Rudi van Eldik,*[b] and Bernt Krebs*[a]

Dedicated to Professor Dirk Walther on the occasion of his 60th birthday

Keywords: Iron(III) / Peroxo Complexes / Kinetics / Hydrogen Peroxide / Catalase

The new diiron complex $[Fe_2(tbpo)\{O_2As(CH_3)_2\}(CH_3O)(CH_3OH)](ClO_4)_3 \cdot 5\ CH_3OH \cdot 2\ H_2O$ (**1**) containing a (μ-alkoxo)(μ-dimethylarsinato)diiron(III) core was synthesized using the heptadentate ligand *N*,*N*,*N*′,*N*′-Tetrakis(2-benzimidazolylmethyl)-1,3-diamino-2-propanol (Htbpo). The complex was characterized structurally by X-ray crystallography. **1** reproduces the coordination mode and the stoichiometry of the proposed purple acid phosphatase-arsenate inhibitor complex. More importantly, **1** is a good functional model for the activation of small molecules, since the solvent molecule in the coordination sphere of each iron ion can be substituted very easily by a small substrate molecule. This is confirmed by the comparatively high pH-dependent catalase-like activity of **1**. In order to study the influence of the cacodylate bridge on the formation of the metastable adduct with hydrogen peroxide, the analogous hydroxo-bridged complex $[Fe_2(tbpo)(OH)(NO_3)_2](NO_3)_2 \cdot CH_3OH \cdot 2\ H_2O$ (**2**) was employed. The reactions of **1** and **2** with H_2O_2 were studied as a function of $[H_2O_2]$, pH, temperature, and pressure, and the kinetic results including the activation parameters are reported. In the case of compound **2** the reaction proceeds in one step, and the observed first order rate constant, k_{obs}, shows a linear dependence on the hydrogen peroxide concentration with a zero intercept. For complex **1** the kinetic traces could be fitted to two exponential functions. One of the observed pseudo-first-order rate constants, k_{obs1}, exhibits a linear dependence on the hydrogen peroxide concentration with a zero intercept, whereas the other rate constant, k_{obs2}, was independent of the hydrogen peroxide concentration. A mechanistic interpretation is presented.

Introduction

Bridged diiron complexes can be regarded as structural and functional models for non-heme iron proteins.[1−5] Proteins belonging to this class include hemerythrin (Hr), ribonucleotide reductase (RR), methane monooxygenase (MMO), and purple acid phosphatase (PAP), whose X-ray structures are all available.[6−9] The spectroscopic and structural properties of the diiron centres of the metalloproteins have been modelled successfully by using various ligand systems.[10−16] There has been a particular interest in the oxygen activation at these diiron active sites in the last few years.[17−20] Therefore, the reaction of diiron complexes with either dioxygen or hydrogen peroxide has been studied very intensively.[21−24]

Recently, the structures of three dinuclear peroxo bridged iron complexes have been published, which were all generated by the reaction of dioxygen and the diferrous precursor compounds: $[Fe_2(O_2)(C_6H_5CH_2COO)_2\{(HB(pz')_3\}_2]$, $[Fe_2(N\text{-Et-tbpo})(O_2)(Ph_3PO)_2]^{3+}$, and $[Fe_2(Ph\text{-bimp})(C_6H_5COO)(O_2)]^{2+}$.[25−27] These peroxo complexes all show a μ-1,2-binding mode of the introduced peroxo ligand. The (1:1) peroxo adduct of $[Fe_2(tbpo)(OH)(NO_3)_2](NO_3)_2$ was described earlier in the literature,[28] but no X-ray structure was determined. The spectroscopic, magnetic and electrochemical investigations revealed a similar μ-1,2 coordination of the peroxide.

In this work we report the X-ray structure and catalase-like activity of the new μ-arsinato bridged diiron(III) complex $[Fe_2(tbpo)\{O_2As(CH_3)_2\}(CH_3O)(CH_3OH)](ClO_4)_3 \cdot 5\ CH_3OH \cdot 2\ H_2O$ (**1**) containing the heptadentate ligand *N*,*N*,*N*′,*N*′-Tetrakis(2-benzimidazolylmethyl)-1,3-diamino-2-propanol (Htbpo). In order to understand the rapid formation of the μ-peroxo complexes we carried out detailed kinetic studies on the reaction of species **1** and the related, well characterized species $[Fe_2(tbpo)(OH)(NO_3)_2](NO_3)_2 \cdot CH_3OH \cdot 2\ H_2O$ (**2**) with hydrogen peroxide in aqueous solution. The activation parameters for this reaction were determined and plausible mechanisms are postulated.

[a] Anorganisch-Chemisches Institut, Universität Münster
Wilhelm Klemm-Strasse 8, 48149 Münster, Germany
Fax: (internat.) + 49-(0)251/8338366
E-mail: krebs@uni-muenster.de
[b] Institut für Anorganische Chemie,
Universität Erlangen-Nürnberg
Egerlandstr. 1, 91058 Erlangen, Germany
Fax: (internat.) + 49-(0)9131/8527387
E-mail: vaneldik@anorganik.chemie.uni-erlangen.de

Supporting information for this article is available on the WWW under http://www.wiley-vch.de/home/eurjic or from the author.

  1434−1948/99/0909−1537 $ 17.50+.50/0

Results and Discussion

Structural Studies on 1

The structure of **1** confirms a (μ-alkoxo)(μ-dimethylarsinato)diiron(III) core. **1** reproduces the coordination mode and the stoichiometry of the proposed purple acid phosphatase-oxoanion interaction.[31] Therefore **1** can be regarded as a model complex for the proposed structure of the oxidized arsenate complex of uteroferrin.

The cation of **1** is shown in Figure 1, while relevant bond lengths are collected in Table 1. Each iron ion is four-coordinated by the heptadentate ligand $tbpo^-$.

The metal ions are bound by two benzimidazole moieties, one tertiary non-aromatic nitrogen atom and the bridging oxygen atom. The metal centre in **1** exhibits a μ-alkoxo bridged diiron(III) unit with an additional dimethylarsinato bridge. The environments of the ions are completed by the coordination of one methanol and one methanolate ligand. The distance between the methanolic oxygens O4 and O5 (2.452 Å) indicates a strong "hydrogen bridge bond". The proton is assumed to be positioned between O4 and O5 at the same distance to each oxygen atom, so that it can be considered to be delocalized.

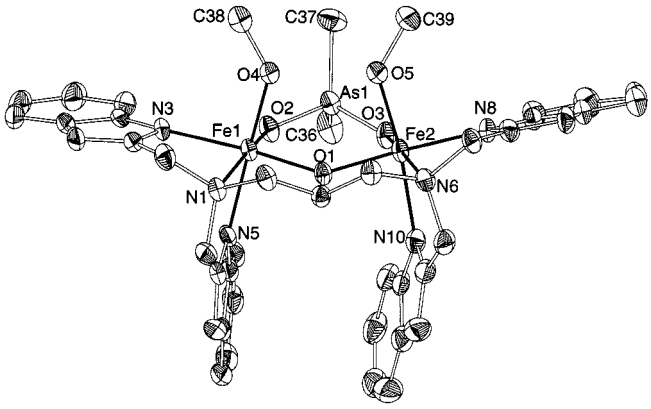

Figure 1. Structure of the cation in **1** showing 50% probability ellipsoids; hydrogen atoms have been omitted for clarity

Table 1. Selected bond lengths [Å] in **1**

Fe(1)···Fe(2)	3.445(1)	O(4)···O(5)	2.452(4)
Fe(1)···As	3.290(1)	Fe(2)···As	3.209(1)
Fe(1)−O(1)	1.941(3)	Fe(2)−O(1)	1.985(3)
Fe(1)−O(2)	1.894(3)	Fe(2)−O(3)	1.874(3)
Fe(1)−O(4)	1.993(3)	Fe(2)−O(5)	1.997(3)
Fe(1)−N(1)	2.293(4)	Fe(2)−N(6)	2.235(4)
Fe(1)−N(3)	2.032(3)	Fe(2)−N(8)	2.033(3)
Fe(1)−N(5)	2.091(4)	Fe(2)−N(10)	2.118(4)
As−O(2)	1.678(3)	As−O(3)	1.652(3)
As−C(36)	1.887(5)	As−C(37)	1.901(5)

Only two complexes containing a (μ-alkoxo)(μ-dimethylarsinato)diiron(III) core are known.[23] The Fe···Fe distance in **1** of 3.445 Å is shorter than the metal-metal separation in $[Fe_2(tbpo)\{O_2As(CH_3)_2\}(Cl)(H_2O)]^{3+}$ (3.58 Å)[23b] and $[Fe_2(mtbpo)\{O_2As(CH_3)_2\}(Cl)_2\ (CH_3OH)]^{2+}$ (3.54 Å)[23a]. The average Fe···As separation in **1** (3.25 Å) is in accordance with the Fe···As distances in $[Fe_2(tbpo)\{O_2As(CH_3)_2\}(Cl)(H_2O)]^{3+}$ and $[Fe_2(mtbpo)\{O_2As(CH_3)_2\}(Cl)_2(CH_3OH)]^{2+}$ with 3.31 Å and 3.28 Å, respectively.

Functional Studies on 1 and 2

The evolution of dioxygen was measured to investigate the hydrogen peroxide decomposition by complexes **1** and **2**. Figure 2 shows the initial decomposition rate after addition of the complexes **1**, **2**, or iron(III) salts (blind) to buffered aqueous hydrogen peroxide solutions. Both complexes exhibit only very little activity at pH 5 to 7 and no activity at pH 3 to 4, which is consistent with a completely protonated form of the substrate under these conditions. A little increase is observed at pH 8. The initial rate for the peroxide decomposition (0.90% O_2 per second) of complex **1** at pH 9 shows a significant increase in catalase-like activity at this pH. **2** has also a comparably high activity at pH 9 (0.48% O_2 per second). A solution containing iron(III) perchlorate instead of a complex shows no or very little activity at pH 3 to 9, which is also consistent with low solubility. Logarithm plots of the initial rates versus complex and peroxide concentrations, respectively, indicate that the reaction of **1** and **2** at pH 9 is first order in complex and peroxide concentration.

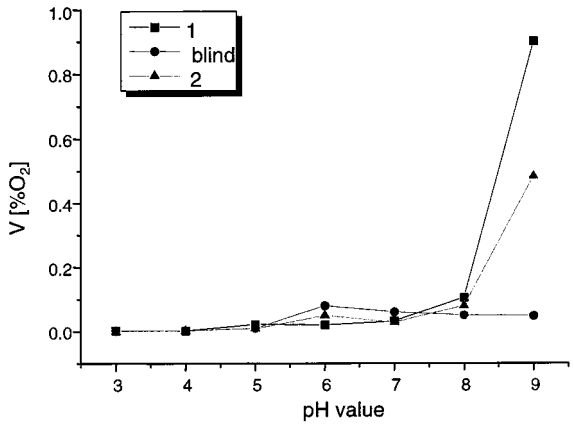

Figure 2. pH-dependence of the catalase-like activity of **1** and **2**

These experiments show that the decomposition of hydrogen peroxide is strongly pH dependent. **1** has approximately twice the activity than **2** to decompose hydrogen peroxide. Both complexes have a significantly higher catalase-like activity than iron(III) at pH 8 and 9. Activity at higher pH values could not be investigated due to solubility problems. **1** and **2** form metastable peroxide adducts at lower pH values. This adduct formation was investigated using kinetic methods.

Kinetic Measurements on the $[Fe_2(tbpo)(OH)(NO_3)_2](NO_3)_2$ Complex 2

A typical series of time resolved spectra observed during the reaction of the $[Fe_2(tbpo)(OH)(NO_3)_2](NO_3)_2$ complex **2** with an excess of hydrogen peroxide is shown in Figure 3.

The formation of the intensively blue coloured and metastabile peroxo species is accompanied by the formation of a new broad absorbance band at 550 nm, which strongly depends on the selected solvent[28] and is assigned to the iron–peroxo charge transfer. All subsequent kinetic measurements were performed at this wavelength.

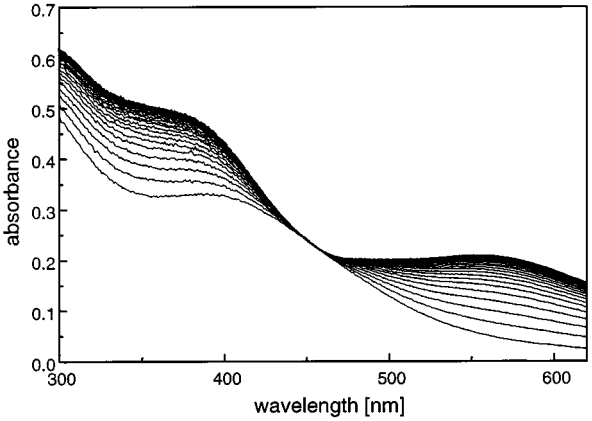

Figure 3. Typical time resolved spectra (10 ms) for the reaction of the hydroxo-bridged complex with a ten fold excess of H_2O_2. Experimental conditions: $[Fe_2(tbpo)(OH)] = 9.45 \cdot 10^{-5}$ M, ionic strength = 0.1 M, pH = 4.0, $T = 25.0$°C.

The reactions were followed for at least 5 half-lives and the kinetic traces, recorded in the presence of an excess of hydrogen peroxide, could all be fitted to a single exponential function under all experimental conditions. The observed pseudo-first-order rate constant, k_{obs}, exhibits a linear dependence on the hydrogen peroxide concentration with a zero intercept (Figure 4). An Eyring analysis of the kinetic data collected over the temperature range 5 to 35°C (Figure 5) allowed the estimation of the activation parameters listed in Table 2.

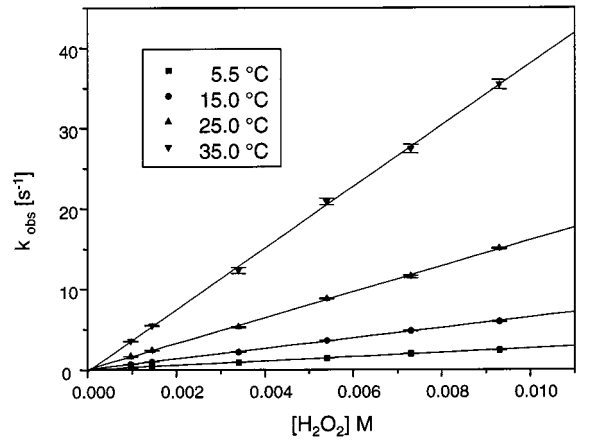

Figure 4. k_{obs} as a function of $[H_2O_2]$ and temperature. Experimental conditions: $[Fe_2(tbpo)(OH)] = 9.45 \cdot 10^{-5}$ M, ionic strength = 0.1 M, pH = 3.0, $T = 5.5–35.0$°C, $\lambda = 550$ nm

Stopped-flow measurements under high pressure showed that the reaction was practically independent of pressure, and the plot of ln k_{obs} vs. pressure gave a zero volume of activation. A preliminary pH dependence study of the reaction was performed in the range 2.0 to 4.0, since the complex showed its lowest catalase-like activity in this pH range. The pH range was limited by the decomposition of the complex occurring at lower pH and the formation of a precipitate at higher pH under the conditions selected for the kinetic measurements. The data showed an increase in the rate constant with increasing pH.

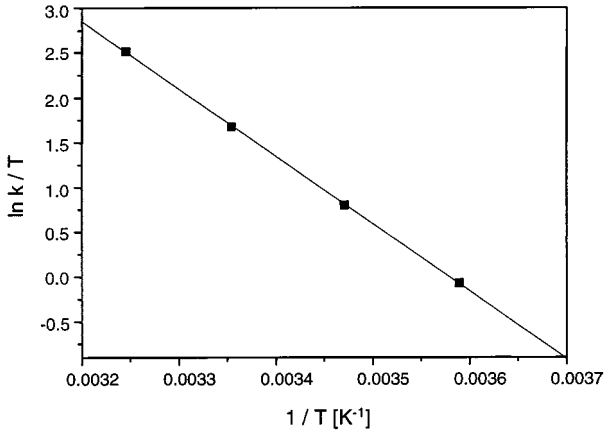

Figure 5. Eyring plot for the reaction of $[Fe_2(tbpo)(OH)]$ ($9.45 \cdot 10^{-5}$ M) with H_2O_2 based on the second-order rate constant determined from the kinetic measurements in the temperature range 5.5–35.0°C

Kinetic Measurements on the $[Fe_2(tbpo)\{O_2As(CH_3)_2\}(OCH_3)(HOCH_3)](ClO_4)_3$ Complex 1

Figure 6 shows a typical series of time resolved spectra observed during the reaction of the $[Fe_2(tbpo)\{O_2As(CH_3)_2\}(OCH_3)(HOCH_3)](ClO_4)_3$ complex with an excess of hydrogen peroxide.

The formation of the intensively blue coloured and metastable peroxo species is accompanied by the formation of a typical broad band at 550 nm, again assigned to the iron–peroxo charge transfer. This wavelength was selected for the kinetic investigations. The reactions were followed for at least 5 half-lives, but in contrast to complex **2** the kinetic traces recorded in the presence of an excess of hydrogen peroxide could not be fitted to a single, but rather to the sum of two exponential functions under all experimental conditions. One of the observed pseudo-first-order rate constants, k_{obs1}, exhibits a linear dependence on the hydrogen peroxide concentration with a zero intercept (Figure 7a), whereas the other rate constant, k_{obs2}, remains independent of the hydrogen peroxide concentration (Figure 7b). An Eyring analysis of the kinetic data collected over the temperature range 5 to 35°C (Figure 8a, b) afforded the activation parameters for k_1 and k_2 listed in Table 2.

The activation volume determined from the pressure dependence studied in the range 5 to 125 MPa is zero within the experimental error limits. The pH dependence was also studied in a preliminary way in the limited range 2.5 to 4.0, for the same reasons as outlined for complex **2**. Both k_{obs1} and k_{obs2} increased with increasing pH.

Table 2. Summary of rate and activation parameters for the reaction of **1** and **2** with H_2O_2 at pH 3.0.

complex	k_2 (s^{-1}) T = 25.0°C	k_1 (M^{-1} s^{-1}) T = 25.0°C	$\Delta H^{\#}$ (kJ mol^{-1})	$\Delta S^{\#}$ (J $mol^{-1}K^{-1}$)	$\Delta V^{\#}$ (cm^3 mol^{-1})
2		1600 ± 40	62.5 ± 0.5	26 ± 17	0 ± 2
1		1820 ± 40	57 ± 2	2 ± 9	0.2 ± 3
1	0.190 ± 0.010		79 ± 4	8 ± 13	−0.3 ± 0.9

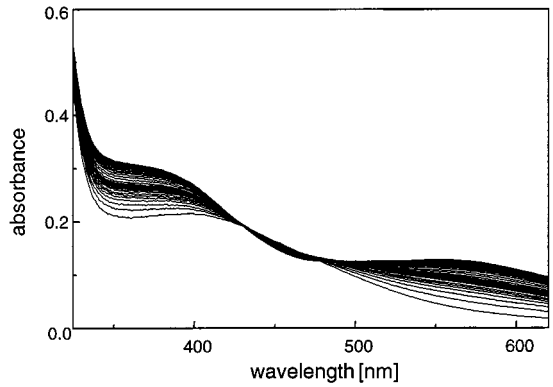

Figure 6. Typical time resolved spectra (10 ms) observed during the reaction of the $[Fe_2(tbpo)\{O_2As(CH_3)_2\}(OCH_3)(HOCH_3)](ClO_4)_3$ **1** complex with a ten fold excess of H_2O_2. Experimental conditions: $[Fe_2(tbpo)(OH)] = 9.45\cdot10^{-5}$ M, ionic strength = 0.1 M, pH = 3.0, T = 25.0°C.

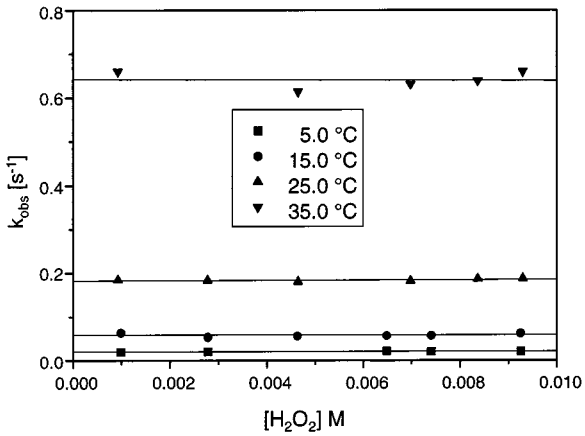

Figure 7b. k_{obs2} as a function of $[H_2O_2]$ and temperature. Experimental conditions: $[Fe_2(tbpo)\{O_2As(CH_3)_2\}] = 9.45\cdot10^{-5}$ M, ionic strength = 0.1 M, pH = 3.0, T = 5.0−35.0°C, λ = 550 nm

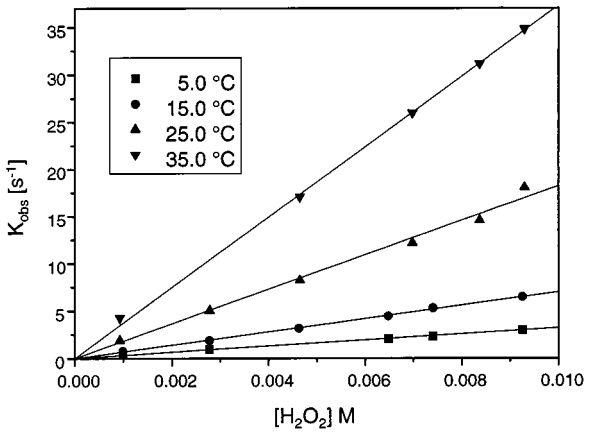

Figure 7a. k_{obs1} as a function of $[H_2O_2]$ and temperature. Experimental conditions: $[Fe_2(tbpo)\{O_2As(CH_3)_2\}] = 9.45\cdot10^{-5}$ M, ionic strength = 0.1 M, pH = 3.0, T = 5.0−35.0°C, λ = 550 nm

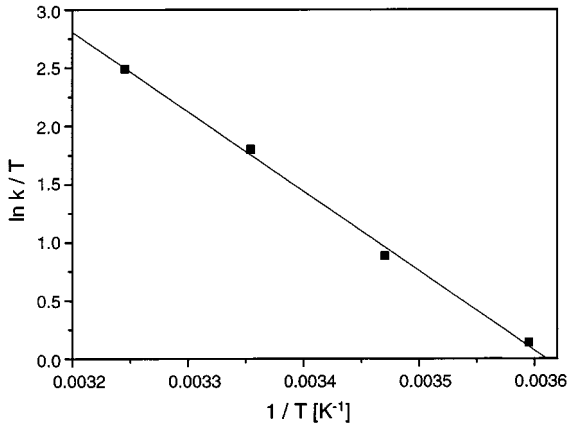

Figure 8a. Eyring plot for the reaction of $[Fe_2(tbpo)\{O_2As(CH_3)_2\}]$ ($9.45\cdot10^{-5}$ M) with H_2O_2 based on the second-order rate constant determined from the kinetic measurements in the temperature range 5.0−35.0°C at pH 3.0

Conclusion

At present no structural information is available on the peroxo products of both complexes **1** and **2.** From the literature[21][28] and our own spectroscopic investigations[32] we know that both complexes form a 1:1 adduct with H_2O_2. For the hydroxo-bridged complex the displacement of the hydroxo bridge during the formation of the peroxo complex is suggested in the literature,[28] whereas for the related benzoate-bridged complex $\{[Fe_2(tbpo)(OBz)](BF_4)_2\}$ no displacement of the benzoate bridge seems to occur.[21] In the X-ray structure of $[Fe_2(tbpo)(OH)(NO_3)_2](NO_3)_2$[33] two nitrates are coordinated to the iron centres, but in aqueous solution it is reasonable to expect that these will be displaced by water molecules. Similarly, in the cacodylate-bridged complex, two water molecules are coordinated to the iron centres, thereby replacing the methanol molecules. pH measurements after addition of two stoichiometrical amounts of acid to the complex solution showed that no protonation of the bridge occurs under these conditions. Spectrophotometric titrations could not be resolved in detail due to the complexity of the system.

The suggested reaction mechanisms for both complexes are shown in Schemes 1 and 2. For both complexes the first step is suggested to be the addition of H_2O_2 to one of the iron centres, which involves substitution of a more labile bond (e.g. coordinated water). In the case of the hydroxo-

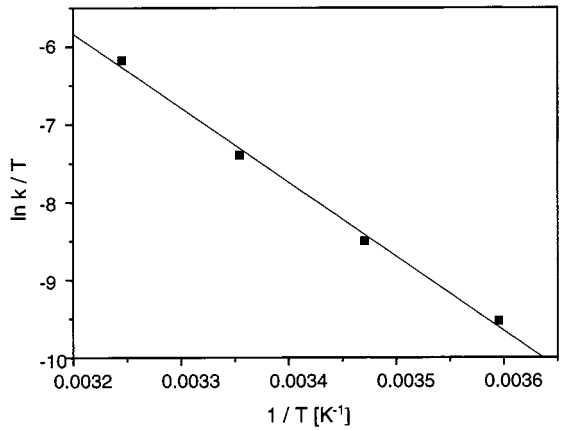

Figure 8b. Eyring plot for the reaction of $[Fe_2(tbpo)\{O_2As(CH_3)_2\}]$ ($9.45 \cdot 10^{-5}$ M) with H_2O_2 based on the first-order rate constant determined from the measurements in the temperature range 5.0−35.0°C at pH 3.0

bridged complex, a very fast ring closure follows which most probably involves the release of the hydroxo-bridge, which can be observed by magnetic and conductivity measurements.[28] In the other case the first reaction is the same, but the subsequent ring-closure reaction is much slower, and so it can be observed in the kinetics as k_2, a $[H_2O_2]$ independent rate constant. Due to the more stable binding of the cacodylate bridge it is not released during the formation of the peroxo adduct. This bulky bridge causes a steric hindrance during the ring-closure reaction, such that this reaction becomes much slower. The rate constant for the first step is similar to the rate constant for the hydroxo-bridged complex (see Table 2).

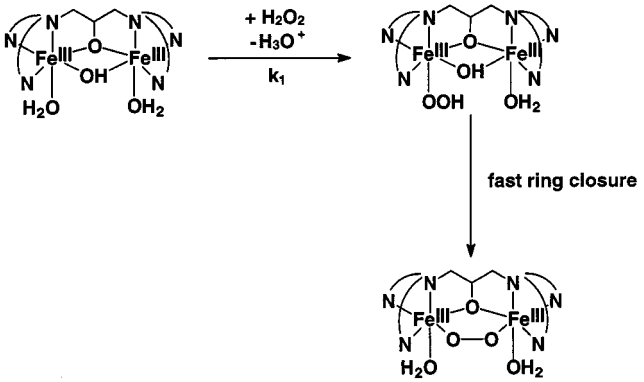

Scheme 1. Suggested mechanism for the reaction of the hydroxo-bridged complex with H_2O_2

The difference between the two complexes concerns the second step of the reaction, i.e. the bridge formation by the hydroperoxo ligand. In the case of the hydroxo-bridged complex the distance between the Fe^{III} centres (3.177 Å) is significantly shorter than in the case of the cacodylate-bridged complex.[33] This is consistent with the rapid bridge-formation step in the former complex and the much slower step in the latter complex.

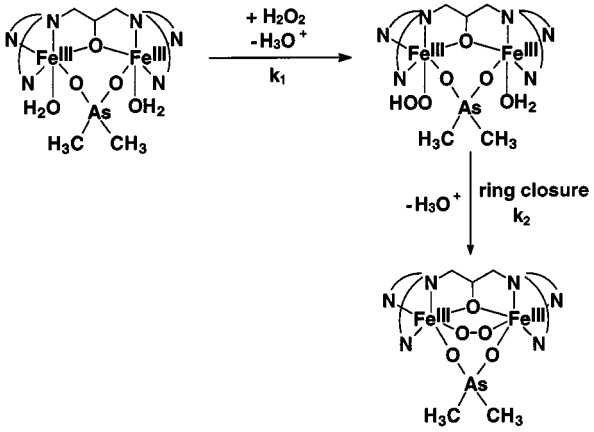

Scheme 2. Suggested mechanism for the reaction of the cacodylate-bridged complex with H_2O_2

For both systems studied, preliminary data showed that the rate constants exhibit an increase with increasing pH over the limited pH range accessible. This can be related to the partial deprotonation of H_2O_2 (pK_a = 11.6), since HO_2^- will be orders of magnitude more nucleophilic than the fully protonated form. In a recent study[34] of the oxidation of hydrogen peroxide by different Ni^{III}, Fe^{III}, and Ru^{III} complexes, the authors also found an increase in the observed rate constants with increasing pH over a similar limited pH range. The data could be fitted to a model in which HO_2^- is up to 7 orders of magnitude more reactive than the fully protonated H_2O_2. A similar explanation can account for our observations, even in the case of the second reaction step observed for the cacodylate complex, since coordinated HO_2^- is expected to have a significantly lower pK_a value than the free ion. Alternatively, it is also possible that another ligand in the coordination sphere undergoes deprotonation at higher pH and results in an increase in reactivity.

The reactions are all characterised by almost zero entropies and volumes of activation. This is typical for a pure interchange substitution mechanism, where coordinated water is displaced during the first step, or by HO_2^- during the second bridge formation step. The similarity in the nature of the donor group and the associated partial molar volumes, can account for the zero volume change observed during the interchange of these ligands in the transition state. Thus the formation of the bridged peroxo complex is controlled by the displacement of the coordinated water molecules in both systems. The similarity in rate constants for the first reaction step indicates that the lability of the coordinated water molecules must be very similar in both complexes. This result also clearly supports the suggested displacement of the nitrate and the methanol/methanolate ligands, respectively, in aqueous solution.

Experimental Section

General Remarks: The heptadentate ligand Htbpo was synthesized as published previously,[23b] while all other chemicals were

Table 3. Crystal structure parameters of **1**

empirical formula	$C_{44}H_{70}N_{10}O_{24}Fe_2AsCl_3$
formula weight [g/mol]	1376.60
crystal system	triclinic
space group	$P\bar{1}$
lattice parameters [(Å) and (deg.)]	a = 12.441(2) α = 70.61(3) b = 13.746(3) β = 74.78(3) c = 19.098(4) γ = 81.16(3)
cell volume [Å^3]	2964.8
Z	2
density [g/cm^3] (calc.)	1.370
radiation	Mo-K_α (λ = 0.71073 Å)
temperature [K]	170
number of collected reflections	13937
number of independent reflections	13312 [R(int = 0.0267)]
number of observed reflections I > 2σ(I)	7445
number of parameters	807
R [$I > 2\sigma(I)$]	$R1$ = 0.0531, $wR2$ = 0.1402
weight	ω = 1/[σ^2(F_o^2) + (0.00731 P)^2+0 P]; P = (F_o+2F_c^2)/3

purchased commercially and used as received. Chemicals of analytical reagent grade and ultrapure water were used throughout this study. **Caution!** The perchlorate salts in this study are potentially explosive and should be handled with care.

Compound **1:** The reaction of equimolar amounts of Htbpo (100 mg) and the sodium salt of cacodylic acid with two equivalents of $Fe(ClO_4)_3 \cdot 9\,H_2O$ in 10 mL of a methanol/ethanol (5:2) solution leads to the formation of red crystals of $[Fe_2(tbpo)\{O_2As(CH_3)_2\}(CH_3O)(CH_3OH)](ClO_4)_3 \cdot 5\,CH_3OH \cdot 2\,H_2O$ (**1**).

Compound **2:** The complex $[Fe_2(tbpo)(OH)(NO_3)_2](NO_3)_2 \cdot CH_3OH \cdot 2\,H_2O$ **2** was synthesized according to literature procedures.[28] The complexes were checked by elemental analysis (CHN-O Rapid, Heraeus). − **1** ($C_{44}H_{70}AsCl_3Fe_2N_{10}O_{24}$): calcd. C 38.39, H 5.31, N 10.17; found C 38.18, H 5.10, N 10.31. − **2** ($C_{36}H_{43}Fe_2N_{14}O_{17}$): calcd. C 41.04, H 3.92, N 18.61; found: C 41.01, H 3.86, N 18.38.

For the kinetic studies both complexes **1** and **2** were dissolved in water and the ionic strength was adjusted with $NaClO_4$ or with $NaNO_3$. The pH of the solution was adjusted with NaOH, $HClO_4$, or HNO_3 and HEPES(I) was used as non-coordinating buffer. Hydrogen peroxide solutions were prepared from 30% hydrogen peroxide and standardized by titration with $KMnO_4$.

Crystallographic Studies:[35] The crystallographic data were collected on a Siemens P3/V diffractometer using monochromated Mo-K_α (λ = 0.71073 Å) radiation by the ω-scan method at 170 K. The crystal of **1** had approximate dimensions of 0.20 × 0.18 × 0.15 mm. Two standard reflections were measured every 99 reflections and remained constant throughout the data collection. The structure was solved using Patterson methods without absorption correction. All non-hydrogen atoms of the cation were refined anisotropically with the SHELX program suite.[36] Refinement was carried out on F^2 using full-matrix least-squares procedures. Hydrogen atoms were included with fixed distances and isotropic temperature factors 1.2 times those of their attached atoms. The R values are defined as $R_1 = \Sigma|F_o - F_c|/\Sigma F_o$ and $wR_2 = [\Sigma[w(F_o^2 - F_c^2)^2/\Sigma[w(F_o^2)^2]]^{1/2}$. Pertinent crystallographic details for **1** are collected in Table 3, and selected bond lenghts are tabulated in Table 1.

Functional Studies: The catalase-like activity measurements were done using a fiberoptical sensor (MOPS, microprocessor-controlled, optical, and portable oxygen sensor), which is based on fluorescence quenching of tris(4,7-diphenyl-1,10-phenanthroline)ruthenium(II) chloride by oxygen. The MOPS indicates dioxygen evolution as percent dioxygen in solution based on calibrations with saturated and unsaturated solutions. 5 mL of aqueous buffer solutions were saturated with nitrogen and different hydrogen peroxide solutions with concentrations between 0.16 and 0.28 mmol·dm^{-3} were added. The decomposition of hydrogen peroxide starts after the addition of a dioxygen-free methanolic complex solution (between 0.003 and 0.01 mmol·dm^{-3}). All reactions were carried out under nitrogen at room temperature in a 10 cm^3 reactor containing a stirring bar at pH values between 3 and 9 and observed over a 5 minute time periode.

Kinetic Studies: The kinetic experiments were performed on Biologic SFM-3 and Applied Photophysics SX.18MV (Leatherhead, UK) stopped-flow instruments, to which an online data acquisition system was connected. Time resolved spectra were recorded on an Applied Photophysics SX.18MV stopped flow (Leatherhead, UK) equipped with a J&M TIDAS 16−500 diode array spectrophotometer (Aalen, Germany). The kinetic measurements at pressures up to 150 MPa were carried out on a homemade high-pressure stopped-flow unit.[29][30] Data fitting was carried out using OLIS KINFIT (OLIS, Bogart, Georgia, USA) and Applied Photophysics (Leatherhead, UK) software. Complete tables of all rate constants (2 pages) are provided in the Supporting Information.

Acknowledgments

The authors gratefully acknowledge financial support from the Volkswagen Foundation, the Deutsche Forschungsgemeinschaft and the Fonds der Chemischen Industrie.

[1] S. J. Lippard, *Angew. Chem., Int. Ed. Engl*. **1988**, *27*, 344−361.
[2] J. Sanders-Loehr, W. D. Wheeler, A. K. Schiemke, B. A. Averill, T. M. Loehr, *J. Am. Chem. Soc.* **1989**, *111*, 8084−8093.
[3] D. M. Kurtz, Jr., *Chem. Rev.* **1990**, *90*, 585−606.
[4] J. B. Vincent, G. C. Lilley, B. A. Averill, *Chem. Rev.* **1990**, *90*, 1447−1467.
[5] L. Que, Jr., A. E. True, *Prog. Inorg. Chem.* **1990**, *38*, 97−200.
[6] M. A. Holmes, J. Le Trong, S. Turley, L. C. Sieker, R. E. Steinkamp, *J. Mol. Biol.* **1991**, *218*, 583−593.
[7] P. Nordlund, B.-M. Sjöberg, H. Eklund, *Nature* **1990**, *345*, 593−598.
[8] A. C. Rosenzweig, C. A. Frederick, S. J. Lippard, *J. Am. Chem. Soc.* **1993**, *366*, 357−543.
[9] [9a] N. Sträter, T. Klabunde, P. Tucker, H. Witzel, B. Krebs, *Science* **1995**, *268*, 1489−1492. − [9b] N. Sträter, W. N. Lipscomb, T. Klabunde, B. Krebs, *Angew. Chem., Int. Ed. Engl.* **1996**, *35*, 2024−2057.
[10] W. H. Armstrong, A. Spool, G. C. Papaefthymiou, R. B. Frankel, S. J. Lippard, *J. Am. Chem. Soc.* **1984**, *106*, 3653−3667.
[11] K. Wieghardt, K. Pohl, K. Gebert, *Angew. Chem., Int. Ed. Engl.* **1983**, *22*, 727−728.
[12] [12a] H. Toftlund, K. S. Murray, P. R. Zwack, L. F. Taylor, O. P. Anderson, *J. Chem. Soc., Chem. Commun.* **1986**, 191−192. − [12b] P. Gomez-Romero, N. Cassan-Pastor, A. Ben-Hussein, G. B. Jameson, *J. Am. Chem. Soc.* **1988**, *110*, 1988−1990.
[13] [13a] M. Kodera, H. Shimakoshi, M. Nishimura, H. Okawa, S. Iijima, K. Kano, *Inorg. Chem.* **1996**, *35*, 4967−4973. − [13b] H. Nie, S. M. J. Aubin, M. S. Mashuta, C.-C. Wu, J. F. Richardson, D. N. Hendrickson, R. M. Buchanan, *Inorg. Chem.* **1995**, *34*, 2382−2388. − [13c] C. Belle, I. Gautier-Luneau, J.-L. Pierre, C. Scheer, *Inorg. Chem.* **1996**, *35*, 3706−3708. − [13d] E. Lambert, B. Chabut, S. Chardon-Noblat, A. Deronzier, G. Chottard, A. Bousseksou, J.-P. Tuchagues, J. Laugier, M. Bardet, J.-M. Latour, *J. Am. Chem. Soc.* **1997**, *119*, 9424−9437.
[14] R. E. Norman, S. Ya, L. Que, Jr., G. Backes, J. Ling, J. Sanders-Loehr, J. H. Zhang, C. J. O′Connor, *J. Am. Chem. Soc.* **1990**, *112*, 1554−1562.

[15] [15a] R.E. Stenkamp, L. C. Sieker, L. H. Jensen, *J. Am. Chem. Soc.* **1984**, *106*, 618−622. − [15b] E. C. Niederhoffer, J. H. Timmons, A. E. Martell, *Chem. Rev.* **1984**, *84*, 137−203.
[16] [16a] B. Bremer, K. Schepers, P. Fleischhauer, W. Haase, G. Henkel, B. Krebs, *J. Chem. Soc., Chem. Commun.* **1991**, 510−512. − [16b] B. Krebs, K. Schepers, B. Bremer, G. Henkel, E. Althaus, W. Müller-Warmuth, K. Griesar, W. Haase, *Inorg. Chem.* **1994**, *33*, 1907−1914. − [16c] K. Schepers, B. Bremer, B. Krebs, G. Henkel, E. Althaus, B. Mosel, W. Müller-Warmuth, *Angew. Chem., Int. Ed. Engl.* **1990**, *29*, 532−534.
[17] J. M. Bollinger, Jr., D. E. Edmondson, B. H. Huynh, J. Filley, J. R. Norton, J. Stubbe, *Science* **1991**, *253*, 292−298.
[18] K. E. Liu, C. C. Johnson, M. Newcomb, S. J. Lippard, *J. Am. Chem. Soc.* **1993**, *115*, 939−947.
[19] [19a] S. K. Lee, B. G. Fox, W. A. Froland, J. D. Lipscomb, E. Münck, *J. Am. Chem. Soc.* **1993**, *115*, 6450−6451. − [19b] S. K. Lee, J. C. Nesheim, J. D. Lipscomb, *J. Biol. Chem.* **1993**, *268*, 21569−21577. − [19c] K. E. Liu, D. Wang, B. H. Huynh, D. E. Edmondson, A. Salifoglou, S. J. Lippard, *J. Am. Chem. Soc.* **1994**, *116*, 7465−7466. − [19d] K. E. Liu, A. M. Valentine, D. Wang, B. H. Huynh, D. E. Edmondson, A. Salifoglou, S. J. Lippard, *J. Am. Chem. Soc.* **1995**, *117*, 10174−10185.
[20] D. E. Edmonson, B. H. Huynh, *Inorg. Chim. Acta* **1996**, *252*, 399−404.
[21] L. Que, Jr., *J. Chem. Soc., Dalton Trans.* **1997**, 3933−3940.
[22] A. L. Feig, M. Becker, S. Schindler, R. van Eldik, S. J. Lippard, *Inorg. Chem.* **1996**, *35*, 2590−2601.
[23] [23a] B. Eulering, M. Schmidt, U. Pinkernell, U. Karst, B. Krebs, *Angew. Chem., Int. Ed. Engl.* **1996**, *35*, 618−619. − [23b] B. Eulering, F. Ahlers, F. Zippel, M. Schmidt, H.-F. Nolting, B Krebs, *J. Chem. Soc., Chem. Commun.* **1995**, 1305−1307.
[24] [24a] Y. Nishida, M. Takeuchi, H. Shimo, S. Kida, *Inorg. Chim. Acta* **1984**, *96*, 115−119. − [24b] Y. Hayashi, T. Kayatani, H. Sugimoto, M. Suzuki, K. Inomata, A. Uehara, Y. Mizutani, T. Kitagawa, Y. Maeda, *J. Am. Chem. Soc.* **1995**, *117*, 11220−11229. − [24c] R. H. Fish, M. S. Konings, K. J. Oberhausen, R. H. Fong, W. M. Yu, G. Christou, J. B. Vincent, D. K. Coggin, R. M. Buchanan, *Inorg. Chem.* **1991**, *30*, 3002−3006.
[25] K. Kim, S. J. Lippard, *J. Am. Chem. Soc.* **1996**, *118*, 4914−4915.
[26] T. Ookubo, H. Sugimoto, T. Nagayama, H. Masuda, T. Sato, K. Tanaka, Y. Maeda, H. Okawa, Y. Hayashi, A. Uehara, M. Suzuki, *J. Am. Chem. Soc.* **1996**, *118*, 701−702.
[27] Y. Dong, S. Yan, V. G. Young, Jr., L. Que, Jr., *Angew. Chem., Int. Ed. Engl.* **1996**, *35*, 618−620.
[28] B. A. Brennan, Q. Chen, C. Juarez-Garcia, A. E. True, C. J. O′Connor, L. Que, Jr., *Inorg. Chem.* **1991**, *30*, 1937−1943.
[29] R. van Eldik, D. A. Palmer, R. Schmidt, H. Kelm, *Inorg. Chim. Acta* **1981**, *50*, 131.
[30] R. van Eldik, W. Gaede, S. Wieland, J. Kraft, M. Spitzer, D. A. Palmer, *Rev. Sci. Instrum.* **1993**, *64*, 1355.
[31] [31a] A. E. True, R. C. Scarrow, C. R. Randall, R. C. Holz, L. Que, Jr., *J. Am. Chem. Soc.* **1993**, *115*, 4246−4251. − [31b] T. Klabunde, N. Sträter, R. Fröhlich, H. Witzel, B. Krebs, *J. Mol. Biol.* **1996**, *259*, 737−748.
[32] R. Than, L. Westerheide, B. Krebs, unpublished results
[33] J.-R Tzou, S. C. Chang, R. E. Norman, *J. Inorg. Biochem.* **1993**, *51*, 480.
[34] N. Koshino, S. Funahashi, H. D. Takagi, *J. Chem. Soc., Dalton Trans.* **1997**, 4175.
[35] The crystallographic data of the structure reported in this paper were deposited with the Cambridge Crystallographic Data Centre as CCDC-121762. Copies of the data can be obtained free of charge on application to CCDC, 12 Union Road, Cambridge CB2 1EZ, UK (Telefax: Int. +44-1223/336-033 E-mail: deposit@chemcrys.cam.ac.uk).
[36] G. M. Sheldrick, *SHELXS-97* and *SHELXL-97*, Programs for Crystal Structure Determination, Universität Göttingen, **1990** and **1997**.

Received February 26, 1999
[I99068]